Circularly Polarized Dielectric Resonator Antenna with Wide Axial Ratio Bandwidth Using Parasitic Metallic Plates

Partha P. Shome(1), Debanjali Sarkar(2), and Sembiam R. Rengarajan(3)
(1)Department of Electronics and Communication Engineering, SR University, Warangal, India
(2)School of Electronics Engineering, VIT-AP University, Amaravati, India
(3)Department of Electrical and Computer Engineering, California State University, USA

Abstract

The design of a compact dielectric resonator antenna (DRA) with a broad circular polarization (CP) bandwidth is examined in this work. The antenna utilizes a stepped microstrip feeding element coupled via an inverted Z-shaped cross-slot aperture to excite the dielectric resonator effectively. Four carefully rotating curved copper plates encircle the cylindrical dielectric resonator to widen the axial ratio (AR) bandwidth. The cross-slot feed guarantees excellent impedance matching across a broad frequency range, while the interaction between the metallic plates and the dielectric resonator produces tightly spaced AR passbands. With a peak gain of 4.5 dBi within the operating frequency range, the suggested DRA attains an impedance bandwidth of 30% (2.74–3.70 GHz) and an AR bandwidth (ARBW) of 20% (2.7–3.3 GHz).

Keywords- Axial ratio, bandwidth, circular polarization, curved metallic plates, dielectric resonator antenna, wideband

1. Introduction

The DRA has emerged as a versatile and efficient solution for modern wireless communication systems. Unlike conventional metallic antennas, the DRA utilizes a dielectric material as the radiating element, providing several benefits, including reduced losses and high radiation efficiency at microwave and millimeter-wave (mm-Wave) frequencies. Additionally, they provide several advantages, such as simple excitation methods, and flexibility in terms of shape and material [1]. Among various DRA types, those with circular polarization (CP) are particularly favored due to their ability to overcome the misalignment between transmitting and receiving antennas and multipath interference [2]. Consequently, the design of CP DRAs has drawn substantial interest, as highlighted in numerous studies [3-7].

Circular polarization is typically achieved by generating orthogonal degenerate modes within the DRA. In the existing literature, different approaches have been reported for generating CP characteristics in DRAs. CP DRAs can be achieved using stair-shaped slots [8], crossed slots [9-10], or asymmetrical U-slots [11]. In these configurations, the slots need to be orthogonal. Other approaches involve the use of a flat metallic strip [12] or a probe [13]. The paper in [8] presented a modified cylindrical DRA (cDRA) array, achieving wide impedance bandwidth and CP with a 3-dB axial ratio bandwidth (ARBW) of 23.52%. The design enhances gain by 3.0 dBi and demonstrates suitability for WLAN (5.2 GHz) and LTE Band 46 (5.5 GHz) applications. A CP, low-profile, high-gain antenna was proposed in [9] combining features of microstrip patch and dielectric resonator antennas, with a polarization-reconfigurable version supporting RHCP, LHCP, and linear polarization. The authors in [11] investigated a cavity-backed DRA excited by an asymmetrical U-slot for CP. A rectangular DRA excited by a conformal H-shaped metal strip was introduced in [12] achieving broadband CP (~20% bandwidth) and high gain (~6.8 dBic), making it suitable for WiMAX and satellite applications. In [13], a novel technique for broadside CP in a cylindrical DRA is proposed, achieving 51.2% impedance bandwidth and 8.01% ARBW, validated through fabrication and experimental results.

Taking inspiration from existing literature and design approaches, this paper aims to propose a novel CP DRA configuration with a unique approach to achieve ARBW enhancement. This work introduces a novel CP DRA that utilizes parasitic metallic plates to enhance the ARBW while maintaining a simple structure. By allowing a constructive interaction between the dielectric resonator and parasitic metallic plates, the design achieves superior ARBW performance, suitable for next-generation wireless and navigation systems. The remainder of this paper is organized as follows: The proposed antenna design is described in Section. Section 3 presents simulation results to validate the antenna's performance. Finally, Section 4 lists the concluding remarks with future research directions.

2. Antenna Layout

The geometrical representation of the proposed DRA with enhanced ARBW is presented in this section. From Fig. 1, it can be observed that a cylindrical-shaped alumina ($\varepsilon_{ceramic}$ = 9.8; tanδ = 0.002) block is fixed over FR4 substrate (ε_{FR4} = 4.4; tanδ = 0.02). The upper surface of the substrate material is etched with a conducting plane to act as the ground whereas the bottom surface acts as the feeding plane. A stepped microstrip feed line structure feeds the DR through an aperture-coupled structure. The stepped microstrip structure helps to adjust the impedance matching over a wide operating bandwidth. The inverted Z-shaped cross-slot aperture is used as a coupling structure to excite additional resonance in the DR. Four curved parasitic metal blocks are positioned around the cylindrical dielectric resonator to further achieve a wide ARBW.

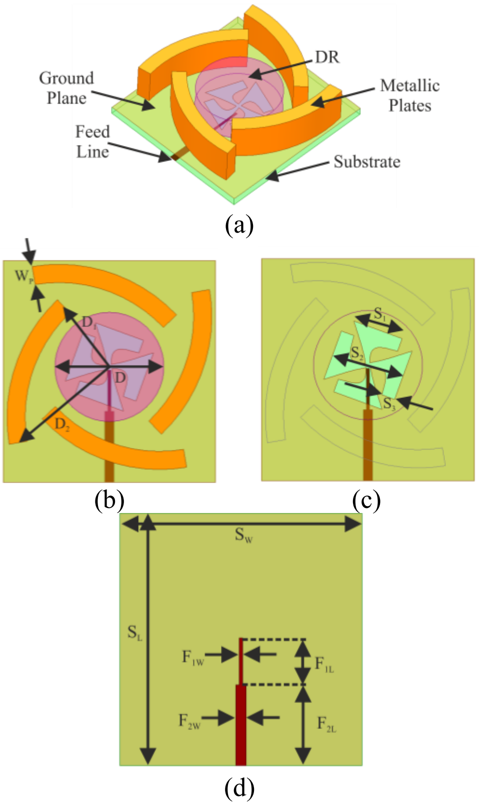

Figure 1 Diagrammatic representation of the suggested wideband CP DRA (a) isometric view, (b) top view, (c) ground-plane view, (d) bottom view

3. Antenna Performance Analysis

This section presents a theoretical analysis of the antenna's performance to provide a clear understanding of the operational mechanism of the proposed DRA. Fig. 2 illustrates the sequential design stages involved in developing the antenna. The performance characteristics at each stage are depicted using the reflection coefficient (|S_{11}|) and axial ratio (AR) curves in Figures 3(a) and 3(b), respectively.

The design process begins with a cylindrical dielectric resonator (CDR) excited by a stepped microstrip line through an inverted Z-shaped cross-slot aperture, forming the initial configuration, referred to as Antenna-1. This configuration exhibits a single narrowband resonance around 3.2 GHz. In the subsequent phase, a slight rotation of the Z-shaped aperture is introduced to enhance the impedance bandwidth, resulting in Antenna-2, which achieves an improved bandwidth range of 2.75–3.43 GHz. To further extend the operational bandwidth, four rectangular metal blocks are positioned around the DR, leading to the development of Antenna-3. This modification also facilitates the creation of a -3 dB AR bandwidth (ARBW). By symmetrically tilting these metal blocks, Antenna-4 is obtained, further enhancing both the impedance bandwidth and ARBW. The final design, Antenna-5, is achieved by incorporating curved metal blocks, which significantly contribute to ARBW improvement. This comprehensive simulation analysis of the proposed DRA highlights the influence of the cross-slot aperture in expanding the impedance bandwidth, while the parasitic metal blocks play a crucial role in ARBW generation and impedance bandwidth control.

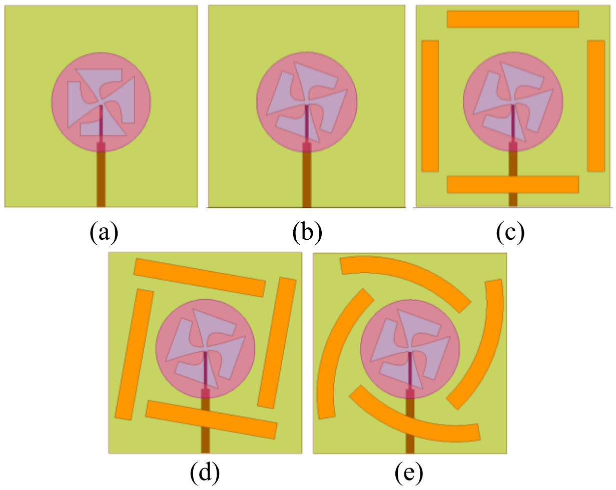

Figure 2 Stages of DRA design evolution (a) Antenna-1, (b) Antenna-2, (c) Antenna-3, (d) Antenna-4, and (e) Antenna-5

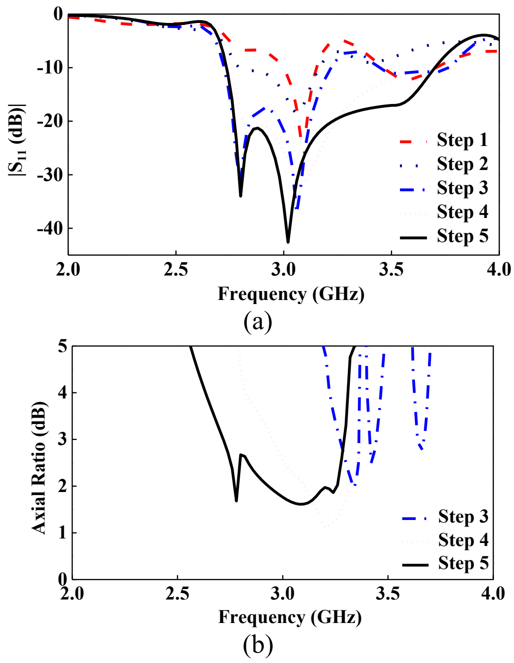

Figure 3 Simulation results of the DRA design stages (a) |S_{11}| and (b) axial ratio

Figure 4 illustrates the surface current distribution across the four curved metallic plates. At a phase of 0° (Fig. 4(a)), the currents in metal blocks 1 and 3 flow in opposite directions along the X-axis, with block 1 in the positive direction and block 3 in the negative direction. Meanwhile, the currents in metal blocks 2 and 4 move in the negative Y-axis direction. Due to the opposing current flow in blocks 1 and 3, their induced electric fields (E-fields) cancel each other out. In contrast, the currents in blocks 2 and 4 are aligned in the same direction, leading to the constructive addition of their induced electric fields. As a result, at a phase of 0°, the net induced electric field produced by the metal block currents is predominantly oriented along the negative Y-axis.

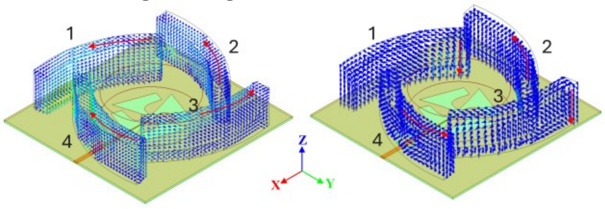

(a) (b)

Figure 4 Simulated surface current distribution on the curved metallic plates at 2.9 GHz (a) at phase 0^0, and (b) at phase 90^0

The currents in the metal blocks reverse direction at a 90° phase. As seen in Fig. 4(b), the currents in metal blocks 1 and 3 flow negatively along the z-axis, whereas the currents in metal blocks 2 and 4 flow positively and negatively along the y-axis, respectively. As a result, the negative Z-axis becomes the primary direction of the E-field produced by the metal block currents during this phase. Since the Y-axis and Z-axis are orthogonal, a pair of orthogonal polarization fields are created with a phase difference of 90^0, thereby enhancing the CP characteristics of the antenna.

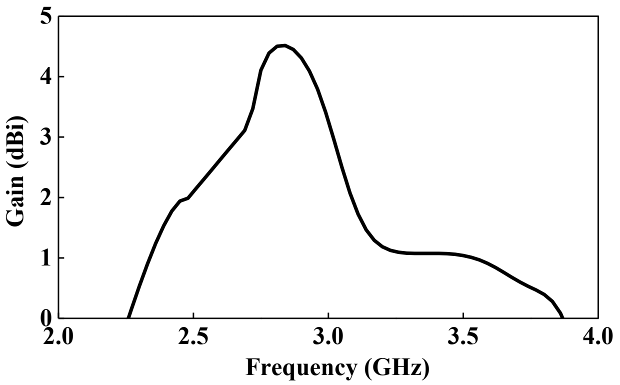

Figure 5 Simulated gain variation as a function of frequency

In Figure 5, the gain of the proposed antenna is displayed. According to the graph, the maximum gain for the designed antenna in the boresight direction is 4.5 dBi. The minor tilt in the direction of maximum radiation is the cause of the antenna's gain decline at the higher end of the bandwidth. This tilt in the radiation pattern is due to the presence of a cross-slot structure in the ground plane of the antenna. Fig. 6 examines and displays the 2-D variation of radiation in the two principal radiating planes. The boresight radiation pattern reveals that the right-hand circularly polarized (RHCP) fields are more dominant than the left-hand circularly polarized (LHCP) fields in both radiation planes, confirming the antenna's strong RHCP performance.

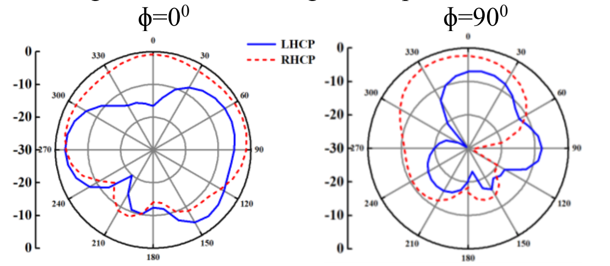

Figure 6 Simulated radiation pattern of the proposed DRA at 2.9 GHz in the far-field region

4. Conclusion

This work successfully investigated the configuration of a novel CP DRA having a wide axial ratio. The design employs parasitic metallic plates strategically placed around a cylindrical dielectric resonator to achieve superior ARBW. The designed antenna achieves an ARBW of 2.7–3.3 GHz and an impedance bandwidth spanning 2.74–3.70 GHz, delivering a peak gain of 4.5 dBi across its operating frequency range. This innovative design provides an alternative to the limitations of conventional CP DRAs and offers a practical solution for modern broadband applications.

References

[1] S. Trinh-Van, Y. Yang, K.-Y. Lee, and K. C. Hwang, "Single-fed circularly polarized dielectric resonator antenna with an enhanced axial ratio bandwidth and enhanced gain," *IEEE Access*, vol. 8, pp. 41045–41052, 2020.

[2] J. Zhu, S. Liao, Y. Yang, S. Li, and Q. Xue, "60 GHz dual-circularly polarized planar aperture antenna and array," *IEEE Trans. Antennas Propag.*, vol. 66, no. 2, pp. 1014–1019, Feb. 2018.

[3] M. Khalily, M. R. Kamarudin, M. Mokayef and M. H. Jamaluddin, "Omnidirectional Circularly Polarized Dielectric Resonator Antenna for 5.2-GHz WLAN Applications," *IEEE Antennas and Wireless Propagation Letters*, vol. 13, pp. 443-446, 2014.

[4] C. C. Lin and J. S. Sun, "Circularly Polarized Dielectric Resonator Antenna Fed by Off-Centered Microstrip Line for 2.4-GHz ISM Band Applications," *IEEE Antennas and Wireless Propagation Letters*, vol. 14, pp. 947-949, Dec. 2015.

[5] X. C. Wang, L. Sun, X. L. Lu, S. Liang, and W. Z. Lu, "Single-feed dual-band circularly polarized dielectric resonator antenna for CNSS applications," *IEEE Trans. Antennas Propag.*, vol. 65, no. 8, pp. 4283–4287, Aug. 2017.

[6] A. Altaf, J. W. Jung, Y. Yang, K. Y. Lee, and K. C. Hwang, "Reconfigurable Dual-/Triple-Band Circularly Polarized Dielectric Resonator Antenna," *IEEE Antennas and Wireless Propagation Letters*, vol. 19, no. 3, pp. 443-447, Mar. 2020.

[7] G. Zhao, Y. Zhou, J. R. Wang and M. S. Tong, "A Circularly Polarized Dielectric Resonator Antenna Based on Quasi-Self-Complementary Metasurface," *IEEE Transactions on Antennas and Propagation*, vol. 70, no. 8, pp. 7147-7151, Aug. 2022.

[8] S. Gupta, A. Sharma, G. Das, R. K. Gangwar, and M. Khalily, "Wideband circularly polarized dielectric resonator antenna array with polarization diversity," *IEEE Access*, vol. 7, pp. 49069–49076, 2019.

[9] W. J. Sun, W. W. Yang, P. Chu, and J. X. Chen, "Design of a wideband circularly polarized stacked dielectric resonator antenna," *IEEE Trans. Antennas Propag.*, vol. 67, no. 1, pp. 591–595, Jan. 2019.

[10] R. Movahedinia, A. R. Sebak, M. R. Chaharmir, M. R. Nikkhah, and A. A. Kishk, "X-band circularly polarized electronically

steerable parasitic array radiator of DRA," *IEEE Trans. Antennas Propag.*, vol. 66, no. 2, pp. 721–728, Feb. 2018.
[11] B. Li, K. K. So, and K. W. Leung, "A circularly polarized dielectric resonator antenna excited by an asymmetrical U-slot with a backing cavity," *IEEE Antennas Wireless Propag. Lett.*, vol. 2, pp. 133–135, 2003.
[12] U. Illahi, *et al.*, "Singly-fed rectangular dielectric resonator antenna with a wide circular polarization bandwidth and beamwidth for WiMAX/Satellite applications," *IEEE Access*, vol. 7, pp. 66206–66214, 2019.
[13] R. Chowdhury, and R. K. Chaudhary, "An approach to generate circular polarization in a modified cylindrical-shaped dielectric resonator antenna using PMC boundary approximation," *IEEE Antennas Wireless Propag. Lett.*, vol. 17, no. 9, pp. 1727–1731, Sep. 2018.